

Classical Communication in the Presence of Quantum Gaussian Noise

Jeffrey H. Shapiro,^a Brent J. Yen,^b Saikat Guha,^a and Baris I. Erkmen^a

^aMassachusetts Institute of Technology, Research Laboratory of Electronics, Cambridge, MA 02139;

^bPrinceton University, Department of Electrical Engineering, Princeton, NJ 08544

ABSTRACT

The classical information capacity of channels that are subject to quantum Gaussian noise is studied. Recent work has established the capacity of the pure-loss channel, as well as bounds on and a conjecture for the capacity of the lossy channel with isotropic-Gaussian excess noise. This work is applied to the pure-loss free-space channel that uses multiple Hermite-Gaussian (HG) or Laguerre-Gaussian (LG) spatial modes to communicate between soft-aperture transmit and receive pupils, and to the lossy channel with anisotropic (colored) Gaussian noise.

Keywords: Channel capacity, quantum Gaussian noise, Hermite-Gaussian modes, Laguerre-Gaussian modes.

1. INTRODUCTION

A principal goal of quantum information theory is evaluating the information capacities of important communication channels. To date, such capacities have only been found for a limited class of channels. In previous work we have found the classical capacity of the pure-loss Bosonic channel,¹ and shown that it is achieved by single-use coherent-state encoding with joint measurements over entire codewords. Single-use coherent-state encoding was also used to obtain a lower bound on the capacity of the thermal-noise channel,^{2,3} which we have shown to be tight in the limits of low and high noise levels. Furthermore, if our conjecture concerning the minimum output entropy of this isotropic Gaussian-noise channel is correct,⁵ then single-use coherent-state encoding is capacity achieving.

In this paper we provide two extensions of our previous work. First, we find the capacity of the pure-loss free-space channel that uses multiple Hermite-Gaussian or Laguerre-Gaussian spatial modes to communicate between soft-aperture transmit and receive pupils. These mode sets are shown to have identical capacity versus transmitter power characteristics, because they share a common set of modal transmissivities. Second, for single-mode communication we study the capacity of the lossy Bosonic channel with anisotropic (colored) Gaussian noise. Here, under the assumption that our minimum output entropy conjecture is correct, we are able to use a noise-whitening argument to find the channel capacity. We begin our development with a brief review of prior classical capacity results for Bosonic channels with isotropic Gaussian noise.

2. BOSONIC CHANNELS WITH ISOTROPIC GAUSSIAN NOISE

We are interested in classical communication over Bosonic channels with propagation loss and Gaussian noise. It is convenient to begin with a treatment at the single-mode level. In this case the channel input is an electromagnetic-field mode with annihilation operator \hat{a} , and its output is another field mode with annihilation operator \hat{a}' . The descriptions of this channel when multiple temporal and/or spatial modes are employed can be built up from tensor-product constructions using the single-mode model. Neither the single-mode nor the multi-mode lossy channels constitute unitary evolutions, so they are governed by trace-preserving completely-positive (TPCP) maps⁶ that relate their output density operators, $\hat{\rho}'$, to their input density operators, $\hat{\rho}$.

The TPCP map $\mathcal{E}_\eta^N(\cdot)$ for the single-mode lossy channel can be derived from the commutator-preserving beam splitter relation

$$\hat{a}' = \sqrt{\eta}\hat{a} + \sqrt{1-\eta}\hat{b}, \quad (1)$$

Send correspondence to J. H. Shapiro, E-mail: jhs@mit.edu, Telephone: 617-253-4179

in which the annihilation operator \hat{b} is associated with an environmental (noise) mode, and $0 < \eta < 1$ is the channel transmissivity. For the pure-loss channel, the \hat{b} mode is in its vacuum state; for the thermal-noise channel this mode is in a thermal state, viz., an isotropic-Gaussian mixture of coherent states with average photon number $N > 0$,

$$\hat{\rho}_b = \int d^2\beta \frac{\exp(-|\beta|^2/N)}{\pi N} |\beta\rangle\langle\beta|. \quad (2)$$

The extension of this model to anisotropic Gaussian noise—and the associated channel capacity analysis for that case—will appear in Sect. 4.

The classical capacity of the single-mode lossy channel is established by random coding arguments akin to those employed in classical information theory. A set of symbols $\{j\}$ is represented by a collection of input states $\{\hat{\rho}_j\}$ that are selected according to some prior distribution $\{p_j\}$. The output states $\{\hat{\rho}'_j\}$ are obtained by applying the channel's TPCP map $\mathcal{E}_\eta^N(\cdot)$ to these input symbols. The Holevo information associated with priors $\{p_j\}$ and states $\{\hat{\sigma}_j\}$ is given by,

$$\chi(p_j, \hat{\sigma}_j) = S\left(\sum_j p_j \hat{\sigma}_j\right) - \sum_j p_j S(\hat{\sigma}_j), \quad (3)$$

where $S(\hat{\sigma}) \equiv -\text{tr}(\hat{\sigma} \ln(\hat{\sigma}))$ is the von Neumann entropy. According to the Holevo-Schumacher-Westmoreland theorem,⁷⁻⁹ the capacity of this channel, in nats per use, is

$$C = \sup_n (C_n/n) = \sup_n \left\{ \max_{\{p_j, \hat{\rho}_j\}} [\chi(p_j, (\mathcal{E}_\eta^N)^{\otimes n}(\hat{\rho}_j))/n] \right\}, \quad (4)$$

where C_n is the capacity achieved when coding is performed over n -channel-use symbols and the supremum over n is necessitated by the fact that channel capacity may be superadditive.

We have previously shown that the capacity of the single-mode, pure-loss channel whose transmitter is constrained to use no more than \bar{N} photons on average is¹

$$C = g(\eta\bar{N}) \text{ nats/use}, \quad (5)$$

where

$$g(x) \equiv (x+1) \ln(x+1) - x \ln(x) \quad (6)$$

is the Shannon entropy of the Bose-Einstein probability distribution. This capacity is achieved by single-use random coding over coherent states using an isotropic Gaussian distribution which saturates the transmitter's bound on average photon number. [Note that the optimality of single-use encoding means that the capacity of the single-mode pure-loss channel is *not* superadditive.] This capacity exceeds what is achievable with homodyne and heterodyne detection,

$$C_{\text{hom}} = \frac{1}{2} \ln(1 + 4\eta\bar{N}) \quad \text{and} \quad C_{\text{het}} = \ln(1 + \eta\bar{N}), \quad (7)$$

although heterodyne detection is asymptotically optimal as $\bar{N} \rightarrow \infty$. An analytical expression for the direct-detection capacity corresponding to this single-mode case is not known, but this capacity has been shown to satisfy,¹⁰

$$C_{\text{dir}} \leq \frac{1}{2} \ln(\eta\bar{N}) + o(1) \quad \text{and} \quad \lim_{\bar{N} \rightarrow \infty} (C_{\text{dir}}) = \frac{1}{2} \ln(\eta\bar{N}), \quad (8)$$

and so is dominated by (5) for $\ln(\eta\bar{N}) > 1$.

For the pure-loss scalar channel in which the transmitter may use all frequencies $\omega \in [0, \infty)$ of a single electromagnetic polarization subject to an average power constraint P with all frequencies having the same channel transmissivity, we have shown that the resulting channel capacity is¹

$$C_{\text{WB}} = \sqrt{\frac{\pi\eta P}{3\hbar}} \text{ nats/sec}, \quad (9)$$

which is $\pi/\sqrt{3}$ times higher than what can be achieved with homodyne or heterodyne detection. Once again, single-use encoding over a coherent-state ensemble is employed, with low frequencies being used preferentially because of the

average power constraint. As yet, there is no corresponding wideband capacity result for direct detection, because existing results^{11, 12} ignore the frequency dependence of photon energy by constraining photon flux rather than power.

For the thermal-noise channel, i.e., the lossy Bosonic channel with isotropic-Gaussian excess noise, we have obtained bounds on the channel capacity. For the sake of brevity, we will restrict our discussion to the single-mode case. A lower bound on the single-mode capacity for this channel is easily obtained. We assume coherent-state encoding over single channel uses with an isotropic Gaussian prior distribution. It then follows that

$$C \geq g(\eta\bar{N} + (1 - \eta)N) - g((1 - \eta)N). \quad (10)$$

We believe that this single-use coherent-state encoding with an isotropic Gaussian prior achieves channel capacity for the thermal-noise channel, i.e., we believe that the right-hand side of Eq. (10) gives the capacity of this channel.³ Because of the following upper bound on the single-mode channel capacity

$$C_n/n \leq \max_{\{p_j, \hat{\rho}_j\}} (S(\hat{\rho}')/n) - \min_{\hat{\rho}_j} (S(\hat{\rho}'_j)/n), \quad \text{where } \hat{\rho}' \equiv \sum_j p_j S(\hat{\rho}'_j) \quad (11)$$

$$= g(\eta\bar{N} + (1 - \eta)N) - \min_{\hat{\rho}_j} (S(\hat{\rho}'_j)/n), \quad (12)$$

the proof of our conjecture is intimately related to the problem of determining the minimum von Neumann entropy that can be realized at the output of the thermal-noise channel by choice of its input state.⁵ So far, among many other things, we have shown that a coherent-state input leads to a *local* minimum in the output entropy, and we have shown that a coherent-state input minimizes the integer-order Rényi output entropies.^{13, 14} A proof of our capacity conjecture would follow immediately from the latter result were a rigorous foundation available for the replica method of statistical mechanics. [The replica method has recently been applied to other problems in communication theory,^{15, 16} so establishing its rigorous basis would have additional import outside of statistical physics and Bosonic-channel communications.] Further support for our output entropy and capacity conjectures comes from the suite of lower bounds that we have obtained on the thermal-noise channel's single-use output entropy.⁵ These bounds provide fairly tight constraints on any possible gap between the channel's minimum output entropy and the associated coherent-state upper bound on this quantity. Indeed these results imply that coherent-state encoding approaches the C_1 capacity at both low and high noise levels. We have also developed numerical results that favor an even stronger conjecture, viz., that the output states resulting from coherent-state inputs to the thermal-noise channel majorize the output states arising from all other inputs.¹³ This majorization conjecture, if true, would immediately imply both the minimum output entropy and the capacity conjectures for the thermal-noise channel.

3. PURE-LOSS FREE-SPACE CHANNEL USING HG OR LG SPATIAL MODES

Although it serves a useful illustrative purpose, the wideband pure-loss channel with frequency-independent loss is not a realistic scenario. Thus we have also studied the far-field, scalar free-space channel in which line-of-sight propagation of a single polarization occurs over an L -m-long path from a circular transmitter pupil (area A_t) to a circular receiver pupil (area A_r) with the transmitter restricted to use frequencies for $\{\omega : 0 \leq \omega \leq \omega_c \ll \omega_0 \equiv 2\pi cL/\sqrt{A_t A_r}\}$. This frequency range is the far-field power transfer regime, wherein there is only a single spatial mode that couples appreciable power from the transmitter pupil to the receiver pupil, and its transmissivity at frequency ω is $\eta(\omega) = (\omega/\omega_0)^2 \ll 1$. Figure 1 shows the geometry, the power allocations versus frequency for heterodyne, homodyne, and optimal reception, and their corresponding capacities versus normalized power, $P_0 \equiv 2\pi\hbar c^2 L^2/A_t A_r$, when only this dominant spatial mode is employed.¹ Because far-field, free-space transmissivity increases as ω^2 , high frequencies are used preferentially for this channel—unlike the case for frequency-independent loss—because the transmissivity advantage of high-frequency photons more than compensates for their higher energy consumption.

We have also explored the near-field behavior of the pure-loss free-space channel,² by employing the full prolate-spheroidal wave function normal-mode decomposition associated with the propagation geometry shown in Fig. 1(a).^{17, 18} Near-field propagation at frequency $\omega = 2\pi c/\lambda$ prevails when $D_f \equiv A_t A_r/(\lambda L)^2$, the product of the transmitter and receiver Fresnel numbers, is much greater than unity. In this case there are approximately D_f spatial modes with near-unity transmissivities, with all other modes affording insignificant power transfer from the transmitter pupil to the receiver pupil. In what follows we shall take another approach to the wideband capacity of the pure-loss free-space channel, by

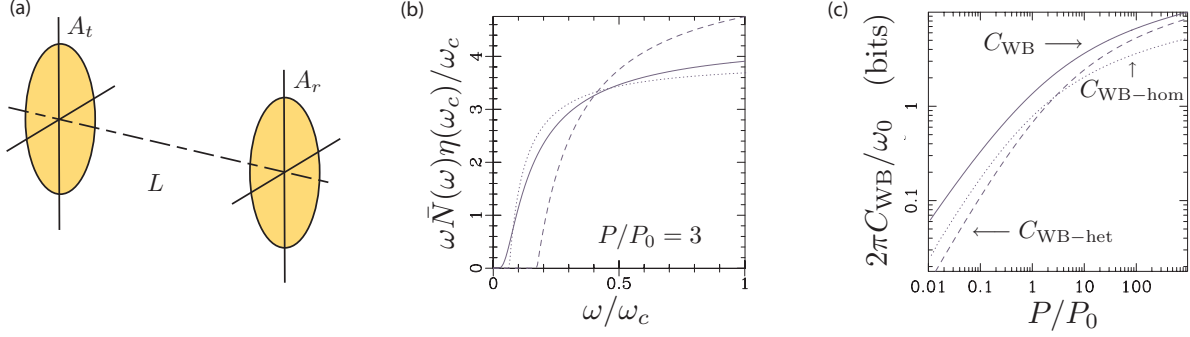


Figure 1. Capacity results for the far-field, free-space, pure-loss channel: (a) propagation geometry; (b) capacity-achieving power allocations $\hbar\omega\bar{N}(\omega)$ versus frequency ω for heterodyne (dashed curve), homodyne (dotted curve), and optimal reception (solid curve), with ω_c and $\hbar\omega_c/\eta(\omega_c)$ being used to normalize the frequency and the power spectra axes, respectively; and (c) wideband capacities of optimal, homodyne, and heterodyne reception versus transmitter power P , with $P_0 \equiv 2\pi\hbar c^2 L^2/A_t A_r$ used for the reference power .

employing either the Hermite-Gaussian (HG) or Laguerre-Gaussian (LG) mode sets that are associated with the soft-aperture (Gaussian-attenuation pupil) version of the Fig. 1(a) propagation geometry. Several benefits will be derived from this approach. First, closed-form expressions become available for the modal transmissivities, as opposed to the hard-aperture Fig. 1(a) case, for which numerical evaluations or analytical approximations must be employed. Second, the LG modes have been the subject of a great deal of interest, in the quantum optics and quantum information communities,¹⁹ owing to their carrying orbital angular momentum. Thus it is germane to explore whether they confer any special advantage in regards to classical information transmission. As we shall see, in the next subsection, the modal transmissivities of the LG modes are isomorphic to those of the HG modes. Inasmuch as the latter do not convey orbital angular momentum, it is clear that such conveyance is not essential to capacity-achieving classical communication over the pure-loss free-space channel.

3.1. Propagation Model: Hermite-Gaussian and Laguerre-Gaussian Mode Sets

In lieu of the hard-aperture propagation geometry from Fig. 1(a), wherein the transmitter and receiver pupils are perfectly transmitting apertures within otherwise opaque planar screens, we now introduce the soft-aperture propagation geometry of Fig. 2. From the quantum version of scalar Fresnel diffraction theory,²⁰ we know that it is sufficient, insofar as this propagation geometry is concerned, to identify a complete set of monochromatic spatial modes—for a single electromagnetic polarization of frequency $\omega = 2\pi c/\lambda = ck$ —that maintain their orthogonality when transmitted through this channel. The resulting two mode sets—i.e., the mode functions at the input and output of the Fig. 2 propagation geometry—constitute a singular-value decomposition (SVD) of the linear propagation kernel (spatial impulse response) associated with this geometry, which we will now develop.

Let $u_i(\vec{x})$, for \vec{x} a 2D vector in the transmitter's exit-pupil plane, denote a frequency- ω field entering the transmitter pupil that is normalized to satisfy

$$\int d^2\vec{x} |u_i(\vec{x})|^2 = 1. \quad (13)$$

The resulting field that leaves the transmitter pupil is taken to be

$$u_T(\vec{x}) = \exp(-|\vec{x}|^2/r_T^2)u_i(\vec{x}), \quad (14)$$

which represents a soft-aperture (Gaussian-attenuation function) spatial truncation. After free-space Fresnel diffraction over an L -m-long path, $u_T(\vec{x})$ produces a field

$$u_R(\vec{x}') = \int d^2\vec{x} u_T(\vec{x}) \frac{\exp(ikL + ik|\vec{x} - \vec{x}'|^2/2L)}{i\lambda L}, \quad (15)$$

in the receiver's entrance-pupil plane, where \vec{x}' is a 2D vector in that plane. The receiver employs a soft-aperture (Gaussian-attenuation function) entrance pupil, so that the field immediately after this pupil is

$$u_o(\vec{x}') = \exp(-|\vec{x}'|^2/r_R^2)u_R(\vec{x}'). \quad (16)$$

Thus, the input-output ($u_i(\vec{x})$ -to- $u_o(\vec{x}')$) relation for the Fig. 2 channel is

$$u_o(\vec{x}') = \int d^2\vec{x} u_i(\vec{x})h(\vec{x}', \vec{x}), \quad (17)$$

where

$$h(\vec{x}', \vec{x}) \equiv \exp(-|\vec{x}'|^2/r_R^2) \frac{\exp(ikL + ik|\vec{x} - \vec{x}'|^2/2L)}{i\lambda L} \exp(-|\vec{x}|^2/r_T^2), \quad (18)$$

is the channel's spatial impulse response.

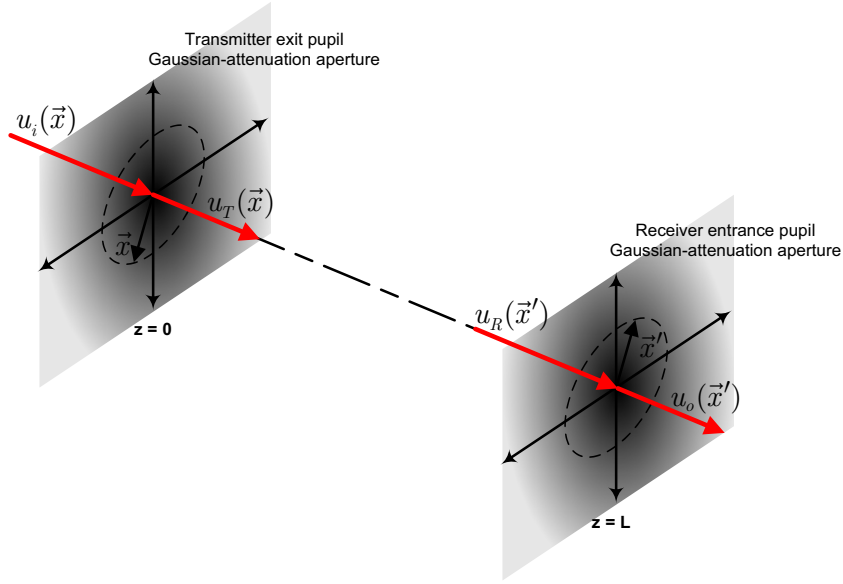


Figure 2. Propagation geometry with soft apertures.

The singular-value (normal-mode) decomposition of $h(\vec{x}', \vec{x})$ is

$$h(\vec{x}', \vec{x}) = \sum_{m=1}^{\infty} \sqrt{\eta_m} \phi_m(\vec{x}') \Phi_m^*(\vec{x}), \quad (19)$$

where

$$1 \geq \eta_1 \geq \eta_2 \geq \eta_3 \geq \dots \geq 0, \quad (20)$$

are the modal transmissivities, $\{\Phi_m(\vec{x})\}$ is a complete orthonormal (CON) set of functions (input modes) on the transmitter's exit-pupil plane, and $\{\phi_m(\vec{x}')\}$ is a CON set of functions (output modes) on the receiver's entrance-pupil plane. Physically, this decomposition implies that $h(\vec{x}', \vec{x})$ can be separated into a countably-infinite set of parallel channels in which transmission of $u_i(\vec{x}) = \Phi_m(\vec{x})$ results in reception of $u_o(\vec{x}') = \sqrt{\eta_m} \phi_m(\vec{x}')$. Singular-value decompositions are unique if their $\{\eta_m\}$ are distinct. When degeneracies exist—i.e., when there are multiple modes with the same η_m value—the SVD is not unique. In particular, a linear combination of input modes with the same η_m value produces $\sqrt{\eta_m}$ times that same linear combination of the associated output modes after propagation through $h(\vec{x}', \vec{x})$. As we shall soon see, owing to singular-value degeneracies, the HG and LG modes of the soft-aperture free-space channel are equivalent mode sets.

The spatial impulse response $h(\vec{x}', \vec{x})$ has both rectangular and cylindrical symmetries. The Hermite-Gaussian modes provide an SVD of this channel that has rectangular symmetry. With $\vec{x} = (x, y)$ in Cartesian coordinates, the HG input modes are as follows:

$$\begin{aligned} \Phi_{n,m}(x, y) &= \frac{\sqrt{2}(1+4\Omega_f)^{1/4}}{r_T \sqrt{\pi n! m! 2^{n+m}}} H_n \left(\frac{\sqrt{2}(1+4\Omega_f)^{1/4}}{r_T} x \right) H_m \left(\frac{\sqrt{2}(1+4\Omega_f)^{1/4}}{r_T} y \right) \\ &\times \exp \left[- \left(\frac{(1+4\Omega_f)^{1/2}}{r_T^2} + i \frac{k}{2L} \right) (x^2 + y^2) \right], \quad \text{for } n, m = 0, 1, 2, \dots, \end{aligned} \quad (21)$$

where $H_p(\cdot)$ is the p th Hermite polynomial and

$$\Omega_f \equiv \frac{kr_T^2}{4L} \frac{kr_R^2}{4L} \quad (22)$$

is the product of the transmitter-pupil and receiver-pupil Fresnel numbers. The modal transmissivities for the HG modes are

$$\eta_{n,m} = \left(\frac{1 + 2\Omega_f - \sqrt{1 + 4\Omega_f}}{2\Omega_f} \right)^{n+m+1}, \quad (23)$$

and the HG output modes are

$$\begin{aligned} \phi_{n,m}(x', y') &= \frac{\sqrt{2}(1+4\Omega_f)^{1/4}}{i^{n+m+1} r_R \sqrt{\pi n! m! 2^{n+m}}} H_n \left(\frac{\sqrt{2}(1+4\Omega_f)^{1/4}}{r_R} x' \right) H_m \left(\frac{\sqrt{2}(1+4\Omega_f)^{1/4}}{r_R} y' \right) \\ &\times \exp \left[- \left(\frac{(1+4\Omega_f)^{1/2}}{r_R^2} - i \frac{k}{2L} \right) (x'^2 + y'^2) \right], \quad \text{for } n, m = 0, 1, 2, \dots, \end{aligned} \quad (24)$$

where $\vec{x}' = (x', y')$. Because channel capacity depends only on the modal transmissivities, it is worth noting that

$$\Omega_f = \sum_{n=0}^{\infty} \sum_{m=0}^{\infty} \eta_{n,m} = \int d^2 \vec{x}' \int d^2 \vec{x} |h(\vec{x}', \vec{x})|^2, \quad (25)$$

where the second equality is a consequence of (19) and the first equality can be obtained either by summing the series or evaluating the double integral. Far-field power transfer occurs when $\Omega_f \ll 1$, in which case $\eta_{0,0} \approx \Omega_f$ and all the other modal transmissivities are insignificantly small in comparison. Near-field power transfer occurs when $\Omega_f \gg 1$, in which case there are many modes that couple appreciable power from the transmitter pupil to the receiver pupil. However, because the HG mode decomposition presumes soft-aperture pupils, the near-field modal transmissivities do not have the abrupt near-unity to near-zero transition that occurs for the hard-aperture singular values.

The HG modes' singular values have degeneracies, i.e., there q HG modes whose modal transmissivities equal $\eta_{0,0}^q$, hence the HG-mode SVD of $h(\vec{x}', \vec{x})$ is not unique. The Laguerre-Gaussian modes provide an alternative SVD for this channel, one with cylindrical rather than rectangular symmetry. Using the polar coordinates $\vec{x} = (r, \theta)$ we have that the LG input modes are

$$\begin{aligned} \Phi_{p,\ell}(r, \theta) &= \sqrt{\frac{2p!}{\pi(|\ell|+p)!}} \frac{(1+4\Omega_f)^{1/4}}{r_T} \left[\frac{\sqrt{2}(1+4\Omega_f)^{1/4}}{r_T} r \right]^{|\ell|} L_p^{|\ell|} \left(\frac{2(1+4\Omega_f)^{1/2}}{r_T^2} r^2 \right) \\ &\times \exp \left[- \left(\frac{(1+4\Omega_f)^{1/2}}{r_T^2} + i \frac{k}{2L} \right) r^2 + i\ell\theta \right], \quad \text{for } p = 0, 1, 2, \dots, \text{ and } \ell = 0 \pm 1, \pm 2, \dots, \end{aligned} \quad (26)$$

where $L_p^{|\ell|}(\cdot)$ is the p th $|\ell|$ th generalized Laguerre polynomial. The corresponding modal transmissivities are given by

$$\eta_{p,\ell} = \left(\frac{1 + 2\Omega_f - \sqrt{1 + 4\Omega_f}}{2\Omega_f} \right)^{(2p+|\ell|+1)}, \quad (27)$$

from which it can be seen that the HG modes with $n + m + 1 = q$ span the same eigenspace as the LG modes with $2p + |\ell| + 1 = q$, and hence are related by a unitary transformation. The LG output modes are

$$\begin{aligned} \phi_{p,\ell}(r', \theta') &= \sqrt{\frac{2p!}{\pi(|\ell| + p)!}} \frac{(1 + 4\Omega_f)^{1/4}}{i^{2p+|\ell|+1} r_R} \left[\frac{\sqrt{2}(1 + 4\Omega_f)^{1/4}}{r_R} r' \right]^{|\ell|} L_p^{|\ell|} \left(\frac{2(1 + 4\Omega_f)^{1/2}}{r_R^2} r'^2 \right) \\ &\times \exp \left[- \left(\frac{(1 + 4\Omega_f)^{1/2}}{r_R^2} - i \frac{k}{2L} \right) r'^2 + i\ell\theta' \right], \quad \text{for } p = 0, 1, 2, \dots, \text{ and } \ell = 0 \pm 1, \pm 2, \dots, \end{aligned} \quad (28)$$

where $\vec{x}' = (r', \theta')$. As was the case for the HG modes, channel capacity when LG modes are employed depends only on the modal transmissivities.

A single frequency- ω photon in the LG mode $\Phi_{p,\ell}(r, \theta)$ carries orbital angular momentum $\hbar\ell$ directed along the propagation (z) axis, whereas that same photon in the HG mode $\Phi_{n,m}(x, y)$ carries no z -directed orbital angular momentum. The equivalence of the $\{\eta_{p,\ell}\}$ and the $\{\eta_{n,m}\}$ then implies that angular momentum does not play a role in determining the ultimate—channel capacity—limit on classical information transmission over the free-space channel shown in Fig. 2.

3.2. Wideband Capacities with Multiple Spatial Modes

Here we shall address the wideband capacities that can be achieved over the pure-loss, scalar free-space channel shown in Fig. 2 using either heterodyne detection, homodyne detection, or optimum (joint measurement over entire codewords) reception. We will allow the transmitter to use multiple spatial modes—from either the HG or LG mode sets—and all frequencies $\omega \in [0, \infty)$ subject to a constraint, P , on the average power in the field entering the transmitter's exit pupil. It follows from our prior work^{1,2} that the capacities we are seeking satisfy,

$$C(P) = \max_{\bar{N}_q(\omega)} \sum_{q=1}^{\infty} q \int_0^{\infty} \frac{d\omega}{2\pi} C_{\text{SM}}(\eta(\omega)^q, \bar{N}_q(\omega)), \quad (29)$$

where the maximization is subject to the average power constraint,

$$P = \sum_{q=1}^{\infty} q \int_0^{\infty} \frac{d\omega}{2\pi} \hbar\omega \bar{N}_q(\omega), \quad (30)$$

and

$$\eta(\omega)^q \equiv \left(\frac{1 + 2\Omega_f - \sqrt{1 + 4\Omega_f}}{2\Omega_f} \right)^q \quad (31)$$

is the modal transmissivity at frequency ω with q -fold degeneracy. In (29),

$$C_{\text{SM}}(\eta, \bar{N}) \equiv \begin{cases} g(\eta\bar{N}), & \text{for optimum reception} \\ \ln(1 + \eta\bar{N}), & \text{for heterodyne detection} \\ \frac{1}{2} \ln(1 + 4\eta\bar{N}), & \text{for homodyne detection} \end{cases} \quad (32)$$

are the relevant single-mode capacities as functions of the modal transmissivity, η , and the average photon number, \bar{N} , for that mode. Regardless of the frequency dependence of $\eta(\omega)$ the single-mode capacity formulas for heterodyne and homodyne detection imply that their wideband multiple-spatial-mode capacities bear the following relationship,

$$C_{\text{hom}}(P) = \frac{1}{2} C_{\text{het}}(4P). \quad (33)$$

Thus, only two maximizations need to be performed—both of which can be done via Lagrange multipliers—to obtain the wideband multiple-spatial-mode capacities for optimum reception, heterodyne detection, and homodyne detection.

The results we have obtained, by performing the preceding maximizations, are shown in Fig. 3. Here we have plotted the heterodyne detection, homodyne detection, and optimum reception capacities in bits/sec, normalized by $\omega_0 =$

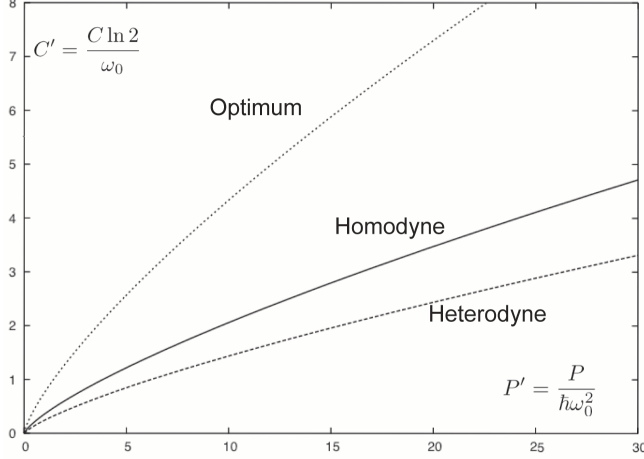


Figure 3. Wideband, multiple-spatial-mode capacities for the scalar, pure-loss, free-space channel that are realized with optimum reception, homodyne detection, and heterodyne detection. The capacities, in bits/sec, are normalized by $\omega_0 = 4cL/r_{TRR}$, the frequency at which $\Omega_f = 1$, and plotted versus the average transmitter power normalized by $\hbar\omega_0^2$.

$4cL/r_{TRR}$, the frequency at which $\Omega_f = 1$, versus the normalized power, $P/\hbar\omega_0^2$. Unlike the case seen in Fig. 1(c) for the wideband capacities of the single-spatial-mode, far-field pure-loss channel—in which heterodyne detection outperforms homodyne detection at high power levels—Fig. 3 shows that homodyne detection is consistently better than heterodyne detection for the multiple-spatial-mode scenario. This behavior has a simple physical explanation. Consider first the single-spatial mode wideband capacities. At low power levels, when capacity is power limited, homodyne detection outperforms heterodyne detection because at every frequency it suffers less noise. On the other hand, at high enough power levels single-spatial mode communication becomes bandwidth limited. In this case heterodyne detection’s factor-of-two bandwidth advantage over homodyne detection carries the day. Things are different when multiple spatial modes are available. In this case, increasing power never reaches bandwidth-limited operation; additionally, lower transmissivity, spatial modes get employed as the power is increased so that the noise advantage of homodyne detection continues to give a higher channel capacity than does heterodyne detection.

Figure 3 shows that the wideband capacity realized with optimum reception, on the multiple-spatial-mode pure-loss channel, increasingly outstrips that of homodyne detection with increasing transmitter power. This advantage indicates that joint measurements over entire codewords—which are implicit in the Holevo information maximization procedure that leads to the optimum-reception capacity—afford performance that is unapproachable with homodyne detection, which is a single-use quantum measurement.

4. BOSONIC CHANNELS WITH ANISOTROPIC GAUSSIAN NOISE

We now return to the single-mode case, and generalize our previous work on lossy Bosonic channels with Gaussian excess noise to include anisotropic (colored) noise. Some multi-mode results for the lossy channel with anisotropic-Gaussian excess noise appear elsewhere.⁴

The channel mode we shall consider is the TPCP map, $\mathcal{E}_\eta^{\mathbf{V}_b}(\cdot)$, associated with the beam splitter relation (1), when the noise mode, \hat{b} , is in a zero-mean Gaussian state whose density operator, $\hat{\rho}_b$, is completely characterized by its quadrature covariance matrix,

$$\mathbf{V}_b \equiv \begin{bmatrix} \langle \hat{b}_1^2 \rangle & \langle \hat{b}_1 \hat{b}_2 + \hat{b}_2 \hat{b}_1 \rangle / 2 \\ \langle \hat{b}_1 \hat{b}_2 + \hat{b}_2 \hat{b}_1 \rangle / 2 & \langle \hat{b}_2^2 \rangle \end{bmatrix}, \quad (34)$$

where $\hat{b}_1 \equiv \text{Re}(\hat{b})$ and $\hat{b}_2 \equiv \text{Im}(\hat{b})$ are the quadrature components of \hat{b} . Isotropic Gaussian noise, as encountered in the thermal-noise channel, has

$$\mathbf{V}_b = \frac{2\langle \hat{b}^\dagger \hat{b} \rangle + 1}{4} \mathbf{I}, \quad (35)$$

where \mathbf{I} is the 2×2 identity matrix. All other valid covariance matrices imply that the noise is anisotropic.

In seeking the capacity of this channel, we shall *assume* that our conjectures about the capacity and minimum output entropy of the thermal-noise (isotropic-Gaussian noise) channel are correct. Presuming the correctness of those conjectures, we now have the following theorem.

THEOREM 4.1. *The channel capacity of the Gaussian-noise channel $\mathcal{E}_\eta^{\mathbf{V}_b}(\cdot)$ is given by*

$$C = g(\eta\bar{N} + (1 - \eta)N_b) - g((1 - \eta)(2|\mathbf{V}_b|^{1/2} - 1/2)), \quad (36)$$

when the average photon number constraint on the transmitter satisfies $\bar{N} \geq N_{\text{thresh}}$, where

$$\bar{N}_{\text{thresh}} \equiv \frac{1}{\eta} \sqrt{(V'_{11} - V'_{22})^2 + 4V'^2_{12}} + V_{11} + V_{22} - 1/2, \quad (37)$$

$$\mathbf{V}' \equiv \eta\mathbf{V} + (1 - \eta)\mathbf{V}_b, \quad (38)$$

$$\mathbf{V} \equiv \frac{1}{4} \begin{bmatrix} |\mu + \nu|^2 & 2\text{Im}(\mu\nu) \\ 2\text{Im}(\mu\nu) & |\mu - \nu|^2 \end{bmatrix}, \quad (39)$$

$N_b \equiv \langle \hat{b}^\dagger \hat{b} \rangle$ is the average photon number of the noise source, and the parameters μ and ν are chosen such that the squeeze operator

$$\hat{S}(\xi) \equiv \exp \left[\frac{\zeta}{2} (e^{-i\gamma} \hat{b}^2 - e^{i\gamma} \hat{b}^{\dagger 2}) \right], \quad (40)$$

with $\xi = \zeta e^{i\gamma}$, $\mu = \cosh(\zeta)$, and $\nu = e^{i\gamma} \sinh(\zeta)$, whitens the Gaussian state $\hat{\rho}_b$.

Proof. We begin by establishing an upper bound on the capacity. From (12), which does not assume that the noise is isotropic, we have that

$$C_n/n \leq g(\eta\bar{N} + (1 - \eta)N_b) - \min_{\hat{\rho}_j} (S(\hat{\rho}'_j)/n). \quad (41)$$

As sketched in Fig. 4, we can use the squeeze operator \hat{S} to find a thermal-noise channel, with TPCP map $\mathcal{E}_\eta^{N_T}(\cdot)$, whose output minimum output entropy is equal to that of our anisotropic noise channel. [In essence, this is the quantum equivalent of the noise-whitening approach to communication through colored noise that is employed in classical communication theory.] The average noise-photon number, N_T , of this equivalent channel is

$$N_T = (2|\mathbf{V}_b|^{1/2} - 1/2), \quad (42)$$

which, when used in conjunction with (41) and our minimum output entropy conjecture, shows that the right-hand side of (36) is an upper bound on the channel capacity.

To show that the right-hand side of (36) is also a lower bound on the channel capacity when $\bar{N} \geq \bar{N}_{\text{thresh}}$, we evaluate the information rate achieved by a single-use squeezed-state code. Let $\hat{\rho}_a^0 = |0; \mu, -\nu\rangle\langle 0; \mu, -\nu|$ be the zero-mean squeezed state whose quadrature-component covariance matrix is given by (39). Consider that random code in which we transmit the displaced squeezed states,

$$\hat{\rho}_a(\alpha) \equiv \hat{D}(\alpha)\hat{\rho}_a^0\hat{D}^\dagger(\alpha), \quad (43)$$

where $\hat{D}(\alpha) \equiv \exp(\alpha\hat{a}^\dagger - \alpha^*\hat{a})$ is the displacement operator, that are selected with a zero-mean Gaussian probability density function whose quadrature-component covariance matrix is denoted \mathbf{V}_a . Imposing the average photon number constraint, $\langle \hat{a}^\dagger \hat{a} \rangle \leq \bar{N}$, assuming that $\bar{N} \geq \bar{N}_{\text{thresh}}$, and applying a capacity result that is due to Holevo, Sohma, and Hirota,²¹ we find that there is a squeezed-state code whose information rate equals the right-hand side of (36).⁴ This implies that

$$C \geq g(\eta\bar{N} + (1 - \eta)N_b) - g((1 - \eta)(2|\mathbf{V}_b|^{1/2} - 1/2)). \quad (44)$$

Equations (41) and (44) provide coincident upper and lower bounds on the capacity, when $\bar{N} \geq \bar{N}_{\text{thresh}}$, hence the proof is complete. \square

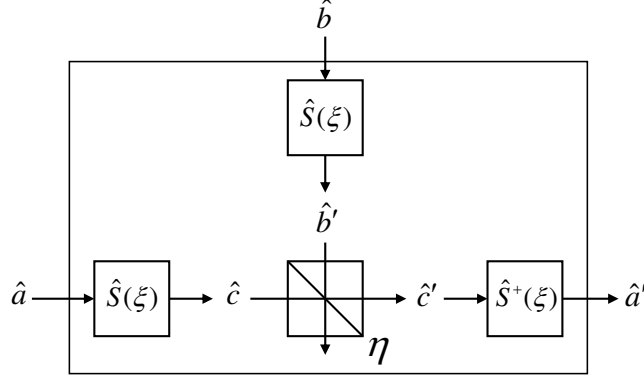


Figure 4. Noise-whitening construction of a thermal-noise channel, $\mathcal{E}_\eta^{N_T}$, that is equivalent to the anisotropic-noise channel $\mathcal{E}_\eta^{\mathbf{V}_b}$. The latter is the \hat{a} -to- \hat{a}' channel; the former is the \hat{c} -to- \hat{c}' channel. The whitening action of the squeeze operator $\hat{S}(\xi)$ puts the \hat{b}' mode into a thermal state with average photon number $N_T = (2|\mathbf{V}_b|^{1/2} - 1/2)$.

There are two special cases of Theorem 4.1 that are worth discussing. First, it is easy to see that when

$$\mathbf{V}_b = \frac{2N_b + 1}{4} \mathbf{I}, \quad (45)$$

$\mathcal{E}_\eta^{\mathbf{V}_b}$ reduces to the thermal-noise channel \mathcal{E}_η^N . Theorem 4.1 then predicts $\bar{N}_{\text{thresh}} = 0$ and $C = g(\eta\bar{N} + (1 - \eta)N) - g((1 - \eta)N)$, in accord with our capacity conjecture for the thermal-noise channel. A more interesting special case occurs when $\hat{\rho}_b = |0; \mu, -\nu\rangle\langle 0; \mu, -\nu|$ is a squeezed state, with $|\nu| > 0$, i.e., a pure-state anisotropic Gaussian noise. Here we find

$$\mathbf{V}' = \mathbf{V} = \mathbf{V}_b = \frac{1}{4} \begin{bmatrix} |\mu + \nu|^2 & 2\text{Im}(\mu\nu) \\ 2\text{Im}(\mu\nu) & |\mu - \nu|^2 \end{bmatrix}, \quad (46)$$

which yields

$$C = g(\eta\bar{N} + (1 - \eta)|\nu|^2), \quad \text{for } \bar{N} \geq \bar{N}_{\text{thresh}} = |\mu\nu|/\eta + |\nu|^2. \quad (47)$$

Note that this capacity is *higher* than that of the thermal-noise channel with the same N value. In other words, phase-sensitive, pure-state Gaussian noise enhances, rather than degrades channel capacity for $\bar{N} \geq \bar{N}_{\text{thresh}}$. Capacity behavior below this average photon number threshold is not known, although partial results are available.⁴

5. CONCLUSIONS

We have reviewed recent work on the capacity of lossy Bosonic channels with isotropic Gaussian noise. We then extended this prior work in two ways. First, for the pure-loss case, we determined the wideband capacity of the free-space channel when multiple Hermite-Gaussian or Laguerre-Gaussian spatial modes are employed. These mode sets are related by unitary transformations over their degenerate eigenspaces, i.e., they have isomorphic modal transmissivities. As a result, they achieve the same capacities, and no fundamental advantage is conferred on classical communication by the fact that the Laguerre-Gaussian modes carry orbital angular momentum. Second, for the single-mode case, we determined the capacity of the lossy channel with anisotropic-Gaussian excess noise in the region above a threshold value on the average photon number of the transmitter, under the assumption that our conjectured capacity for the thermal-noise channel is correct.

ACKNOWLEDGMENTS

This work was supported by the DoD Multidisciplinary University Research Initiative (MURI) program administered by the Army Research Office under Grant DAAD19-00-1-0177.

REFERENCES

1. V. Giovannetti, S. Guha, S. Lloyd, L. Maccone, J. H. Shapiro, and H. P. Yuen, "Classical capacity of the lossy bosonic channel: the exact solution," *Phys. Rev. Lett.* **92**, 027902 (2004).
2. V. Giovannetti, S. Guha, S. Lloyd, L. Maccone, J. H. Shapiro, B. J. Yen, and H. P. Yuen, "Classical capacity of free-space optical communication," *Quantum Information and Computation* **4**, 489–499 (2004).
3. J. H. Shapiro, V. Giovannetti, S. Guha, S. Lloyd, L. Maccone, and B. J. Yen, "Capacity of Bosonic communications," in S. M. Barnett, E. Andersson, J. Jeffers, P. Öhberg, and O. Hirota, eds., *Proceedings of the Seventh International Conference on Quantum Communication, Measurement and Computing* (American Institute of Physics, New York, 2004).
4. B. J. Yen, "Multiple-User Quantum Optical Communication," Research Laboratory of Electronics Technical Report 707, Massachusetts Institute of Technology, October 2004.
5. V. Giovannetti, S. Guha, S. Lloyd, L. Maccone, and J. H. Shapiro, "Minimal output entropy of bosonic channels: a conjecture," *Phys. Rev. A* **70**, 032315 (2004).
6. M. A. Nielsen and I. L. Chuang, *Quantum Computation and Quantum Information* (Cambridge University Press, Cambridge, 2000) Sect. 8.2.4.
7. A. S. Holevo, "The capacity of the quantum channel with general signal states," *IEEE Trans. Inform. Theory* **44**, 269–273 (1998).
8. P. Hausladen, R. Jozsa, B. Schumacher, M. Westmoreland, and W. K. Wootters, "Classical information capacity of a quantum channel," *Phys. Rev. A* **54**, 1869–1876 (1996).
9. B. Schumacher and M. D. Westmoreland, "Sending classical information via noisy quantum channels," *Phys. Rev. A* **56**, 131–138 (1997).
10. A. Lapidoth and S. M. Moser, "Bounds on the capacity of the discrete-time Poisson channel," presented at the 41st Annual Allerton Conference on Communication, Control, and Computing, Monticello, IL, Oct. 2003, <http://www.isi.ee.ethz.ch/moser/publications.shtml>.
11. M. H. A. Davis, "Capacity and cutoff rate for Poisson-type channels," *IEEE Trans. Inform. Theory* **26**, 710–715 (1980).
12. A. D. Wyner, "Capacity and error exponent for the direct detection photon channel—Parts I and II," *IEEE Trans. Inform. Theory* **34**, 1449–1471 (1988).
13. V. Giovannetti, S. Lloyd, L. Maccone, J. H. Shapiro, and B. J. Yen, "Minimum Rényi and Wehrl entropies at the output of Bosonic channels," *Phys. Rev. A* **70**, 022328 (2004).
14. V. Giovannetti and S. Lloyd, "Additivity properties of a Gaussian channel," *Phys. Rev. A* **69**, 062307 (2004).
15. T. Tanaka, "A statistical-mechanics approach to large-system analysis of CDMA multiuser detectors," *IEEE Trans. Inform. Theory* **48**, 2888–2910 (2002).
16. R. R. Miller, "Channel capacity and minimum probability of error in large dual antenna array systems with binary modulation," *IEEE Trans. Signal Process.* **51**, 2821–2828 (2003).
17. D. Slepian, "Prolate spheroidal wave functions, Fourier analysis and uncertainty—IV: extensions to many dimensions; generalized prolate spheroidal functions," *Bell. System Tech. J.* **43**, 3009–3057 (1964).
18. D. Slepian, "Analytic solution of two apodization problems," *J. Opt. Soc. Am.* **55**, 1110–1115 (1965).
19. L. Allen, S. M. Barnett, and M. J. Padgett, eds., *Optical Angular Momentum* (Institute of Physics, Bristol, 2004).
20. H. P. Yuen and J. H. Shapiro, "Optical communication with two-photon coherent states—Part I: quantum state propagation and quantum noise reduction," *IEEE Trans. Inform. Theory*, **24**, 657–668 (1978).
21. A. S. Holevo, M. Sohma, and O. Hirota, "Capacity of quantum Gaussian channels," *Phys. Rev. A* **59**, 1820–1828 (1999).